



1

1 **On the formation of highly oxidized pollutants by autoxidation**
2 **of terpenes under low temperature combustion conditions: the**
3 **case of limonene and α -pinene.**

4 Roland Benoit¹, Nesrine Belhadj^{1,2}, Zahraa Dbouk^{1,2}, Maxence Lailliau^{1,2}, and Philippe Dagaut¹

5 ¹CNRS-INSIS, ICARE, Orléans, France, roland.benoit@cnrs-orleans.fr, nesrine.belhadj@cnrs-orleans.fr,
6 zahraa.dbouk@cnrs-orleans.fr, maxence.lailliau@cnrs-orleans.fr, dagaut@cnrs-orleans.fr

7 ²Université d'Orléans, Orléans, France

8 **Correspondence:** Roland Benoit (roland.benoit@cnrs-orleans.fr)

9 **Abstract.**

10 The oxidation of monoterpenes under atmospheric conditions has been the subject of numerous studies. They were
11 motivated by the formation of oxidized organic molecules (OOM) which, due to their low vapor pressure,
12 contribute to the formation of secondary organic aerosols (SOA). Among the different reaction mechanisms
13 proposed for the formation of these oxidized chemical compounds, it appears that the autoxidation mechanism,
14 involving successive events of O₂ addition and H-migration, common to both low-temperature combustion and
15 atmospheric conditions, is leading to the formation of highly oxidized products (HOPs). However, cool flame
16 oxidation (~500-800 K) of terpenes has not received much attention even if it can contribute to atmospheric
17 pollution through biomass burning and wildfires. Under such conditions, terpenes can be oxidized via autoxidation.
18 In the present work, we performed oxidation experiments with limonene-oxygen-nitrogen and α -pinene-oxygen-
19 nitrogen mixtures in a jet-stirred reactor (JSR) at 590 K, a residence time of 2 s, and atmospheric pressure.
20 Oxidation products were analyzed by liquid chromatography, flow injection, and soft ionization-high resolution
21 mass spectrometry. H/D exchange and 2,4-dinitrophenyl hydrazine derivatization were used to assess the presence
22 of OOH and C=O groups in oxidation products, respectively. We probed the effects of the type of ionization used
23 in mass spectrometry analyses on the detection of oxidation products. Heated electrospray ionization (HESI) and
24 atmospheric pressure chemical ionization (APCI), in positive and negative modes were used. We built an
25 experimental database consisting of literature data for atmospheric oxidation and presently obtained combustion
26 data for the oxidation of the two selected terpenes. This work showed a surprisingly similar set of oxidation
27 products chemical formulas, including oligomers, formed under the two rather different conditions, i.e., cool flame
28 and simulated atmospheric oxidation. Data analysis indicated that a subset of chemical formulas is common to all
29 experiments independently of experimental conditions. Finally, this study indicates that more than 45% of the
30 detected chemical formulas in this full dataset can be ascribed to an autoxidation reaction.

31



2

32 1 Introduction

33 Terpenes are emitted into the troposphere by vegetation (Seinfeld and Pandis, 2006). They can be used as drop in
34 fuels (Harvey et al., 2010; Mewalal et al., 2017; Harvey et al., 2015) which could increase emissions via fuel
35 evaporation and unburnt fuel release. Biomass burning and wildfires can also release terpenes and their products
36 of oxidation into the troposphere (Gilman et al., 2015; Hatch et al., 2019). Wildfires temperature ranges from 573
37 to 1373 K (Wotton et al., 2012), which covers both the cool flame (~500-800 K) and intermediate to high
38 temperature combustion regimes. Products of biomass burning have been characterized earlier (Smith et al., 2009).
39 Using van Krevelen diagrams, the authors reported H/C versus O/C in the ranges 0.5 to 3 and 0 to 1, respectively.
40 Whereas a large fraction of these products can derive from cellulose, hemicellulose, and lignin oxidation, their
41 formation via terpenes oxidation cannot be ruled out. In a more recent study (Gilman et al., 2015), it was reported
42 that biomass burning emissions were dominated by oxidized organic compounds (57 to 68% of total mass
43 emissions). Wildfires are getting more and more frequent and their intensity increases. In large wildfires, there are
44 many updrafts which can transport a variety of materials ranging from gases to particulates, and even bacteria
45 (Kobziar et al., 2018). Furthermore, it was recently demonstrated that recent wildfires in Australia produced smoke
46 which could reach an altitude of 35 km (Khaykin et al., 2020). Such events could contribute to ozone destruction
47 (Bernath et al., 2022) but also to tropospheric pollution.

48 Cool flame oxidation is dominated by autoxidation (Bailey and Norrish, 1952; Benson, 1981; Cox and Cole,
49 1985; Korcek et al., 1972) which involves peroxy radicals (ROO[•]). Autoxidation is based on an H-shift and oxygen
50 addition which starts with the initial production of ROO[•] radicals. This mechanism can repeat itself several times
51 and lead to recurrent oxygen additions to form highly oxidized products (Wang et al., 2017; Wang et al.,
52 2018; Belhadj et al., 2020; Belhadj et al., 2021a; Belhadj et al., 2021b): R[•] + O₂ ⇌ ROO[•] (first O₂-addition); ROO[•]
53 ⇌ QOOH (H-shift); QOOH + O₂ ⇌ OOQOOH (second O₂-addition); OOQOOH ⇌ HOOQOOH (H-shift);
54 HOOQOOH + O₂ ⇌ (HOO)₂QOO[•] (third O₂-addition); (HOO)₂QOO[•] ⇌ (HOO)₂QOOH (H-shift);
55 (HOO)₂QOOH + O₂ ⇌ (HOO)₃QOO[•] (fourth O₂-addition) etc. There, the formation of highly oxidized products
56 (HOPs) was mainly attributed to autoxidation reactions (Belhadj et al., 2021c; Benoit et al., 2021).

57 In atmospheric chemistry, it is only relatively recently that this pathway has been considered (Vereecken et al.,
58 2007; Crounse et al., 2013; Jokinen et al., 2014; Berndt et al., 2015; Jokinen et al., 2015; Berndt et al., 2016; Iyer et al.,
59 2021). Also, it has been identified that highly oxidized molecules (HOMs), a source of secondary organic
60 aerosols (SOA), can result from autoxidation processes (Wang et al., 2021; Tomaz et al., 2021; Bianchi et al., 2019).
61 Modeling studies complemented by laboratory experiments showed that autoxidation mechanisms proceed
62 simultaneously on different ROO[•] radicals leading to the production of a wide range of oxidized compounds in a
63 few hundredths of a second (Jokinen et al., 2014; Berndt et al., 2016; Bianchi et al., 2019). Recent works have
64 shown that, under certain atmospheric conditions, this autoxidation mechanism could be competitive with other
65 reaction pathways involving ROO[•] radicals (Bianchi et al., 2019), e.g., the carbonyl channel (ROO[•] → R_HO +
66 OH), the hydroperoxide channel (ROO[•] + HOO[•] → ROOH + O₂ and RO[•] + OH + O₂), disproportionation reactions
67 (ROO[•] + R'OO[•] → RO[•] + R'O[•] + O₂ and R_HO + R'OH + O₂), accretion reactions (ROO[•] + R'OO[•] → ROOR' +
68 O₂). Similarity, in terms of observed chemical formulas of products from cool flame oxidation of limonene and
69 atmospheric oxidation of limonene has been reported recently (Benoit et al., 2021). The same year, Wang et al.
70 showed that the oxidation of alkanes follows this autoxidation mechanism under both atmospheric and combustion



3

71 conditions (Wang et al., 2021). Also, that work confirmed that internal H-shifts in autoxidation can be promoted
72 by the presence of functional groups, as predicted earlier (Otkjær et al., 2018) for ROO[•] radicals containing OOH,
73 OH, OCH₃, CH₃, C=O, or C=C groups.

74 To further assess the importance of these pathways, available data must be compared along with their experimental
75 specificities. In laboratory studies conducted under simulated atmospheric conditions, oxidation occurs at near-
76 ambient temperatures (250-300 K), at atmospheric pressure, in the presence of ozone and/or [•]OH radicals, the NO₃
77 radical, or the chlorine radical (to name but a few) and with low initial terpene concentrations. In combustion, the
78 [•]OH radical, temperature, and pressure are driving autoxidation. Initial reactant concentrations are generally higher
79 compared to atmospheric conditions, so as to compensate for the absence of ozone and initiate oxidation, since
80 terpenes, as other hydrocarbons, react very slowly with O₂. Rising temperature increases isomerization rates and
81 favors autoxidation, at the expense of other possible reactions of ROO[•] radicals. Indeed, it has been reported earlier
82 that a temperature rise from 250 to 273K does not affect the distribution of HOMs (Quéléver et al., 2019) whereas
83 Tröstl et al. suggested that the distribution of HOMs is affected by temperature, α -pinene or particle concentration
84 (Tröstl et al., 2016). Similarly, the experiments of Huang et al. performed at different temperatures (223 K and
85 296 K) and precursor concentration (α -pinene 0.714 and 2.2 ppm) suggested that the physicochemical properties,
86 such as the composition of the oligomers, can be affected by a variation of temperature (Huang et al., 2018). The
87 broad range of chemical molecules formed and the impact of the experimental conditions on their character
88 remains a subject for atmospheric chemistry as well as for combustion chemistry studies. Whatever the mechanism
89 of aerosols formation, i.e., oligomerization, addition, or accretion, their composition will be linked to that of the
90 initial radical pool (Tomaz et al., 2021).

91 In low-temperature combustion, when the temperature is increased, fuel's autoxidation rate goes through a
92 maximum between 500 and 670 K, depending on the nature of the fuel (Belhadj et al., 2020;Belhadj et al., 2021c).
93 In low-temperature combustion chemistry as in atmospheric chemistry, the oxidation of a chemical compound
94 leads to the formation of several thousands of chemical products which result from successive additions of oxygen,
95 isomerization, accretion, fragmentation, and oligomerization (Benoit et al., 2021;Belhadj et al., 2021b). The
96 exhaustive analysis of chemical species remains, under the current instrumental limitations, impossible. Indeed,
97 this would consist in analyzing several thousands of molecules using separative techniques such as ultra-high-
98 pressure liquid chromatography (UHPLC) or ion mobility spectrometry (IMS) (Krechmer et al., 2016;Kristensen
99 et al., 2016). Nevertheless, it is possible to classify these molecular species, considering only C_xH_yO_z compounds,
100 according to criteria accessible via graphic tools representation such as van Krevelen diagrams, double bond
101 equivalent number (DBE), and average carbon oxidation state (OSc) versus the number of carbon atoms
102 (Kourtchev et al., 2015;Nozière et al., 2015). Such postprocessing of large datasets has the advantage of
103 immediately highlighting classes of compounds or physicochemical properties such as the condensation of
104 molecules (vapor pressure), the large variety of oxidized products (C_xH_yO₁₊₁₅ in the present experiments) and the
105 formation of oligomers (Kroll et al., 2011;Xie et al., 2020).

106 In addition to the recent studies focusing on the first steps of autoxidation, a more global approach, based on the
107 comparison of possible chemical transformations related to autoxidation in low temperature combustion and
108 atmospheric chemistry, is needed for evaluating the importance of autoxidation under tropospheric and low-
109 temperature combustion conditions. In order to study the effects of experimental conditions on the diversity of



4

110 chemical molecules formed by autoxidation, we have selected α -pinene and limonene, two isomeric terpenes
111 among the most abundant in the troposphere (Zhang et al., 2018). Limonene has a single ring structure and two
112 double bonds, one of which is exocyclic. α -pinene has a bicyclic structure and a single endo-cyclic double bond.
113 These two isomers with their distinctive physicochemical characters are good candidates for studying autoxidation
114 versus initial chemical structure and temperature. For α -pinene, in addition to the reactivity of its endo-cyclic
115 double bond, products of ring opening of the cyclobutyl group have been detected (Kurtén et al., 2015; Iyer et al.,
116 2021), which could explain the diversity of observed oxidation products. This large pool of oxidation products is
117 increased in the case of limonene by the presence of two double bonds (Hammes et al., 2019; Jokinen et al., 2015).

118 The present work extends that concerning the oxidation of limonene alone (Benoit et al., 2021). Here, we oxidized
119 α -pinene and limonene in a jet-stirred reactor at atmospheric pressure, excess of oxygen, and elevated temperature.
120 We characterized the impact of using different ionization techniques (HESI and APCI) in positive and negative
121 modes on the pool of detected chemical formulas. The particularities of each ionization mode were analyzed to
122 identify the most suitable ionization technique for exploring the formation of autoxidation products under low
123 temperature combustion. H/D exchange and 2,4-dinitrophenyl hydrazine derivatization were used to assess the
124 presence of hydroperoxy and carbonyl groups, respectively. Chemical formulas detected here and in atmospheric
125 chemistry studies were compiled and tentatively used to evaluate the importance of autoxidation routes under both
126 conditions.

127 2 Experiments

128 2.1 Oxidation experiments

129 The present experiments were carried out in a fused silica jet-stirred reactor (JSR) setup presented earlier (Dagaut
130 et al., 1986; Dagaut et al., 1988) and used in previous studies (Dagaut et al., 1987; Benoit et al., 2021; Belhadj et al.,
131 2021c). We studied separately the oxidation of the two isomers, α -pinene and limonene. As in earlier works (Benoit
132 et al., 2021; Belhadj et al., 2021c), α -pinene (+), 98% pure from Sigma Aldrich and limonene (R)-(+), >97% pure
133 from Sigma Aldrich, were pumped by an HPLC pump (Shimadzu LC10 AD VP) with an online degasser
134 (Shimadzu DGU-20 A3) and sent to a vaporizer assembly where it was diluted by a nitrogen flow. Each terpene
135 isomer and oxygen, both diluted by N_2 , were sent separately to a 42 mL JSR to avoid oxidation before reaching 4
136 injectors (nozzles of 1 mm I.D.) providing stirring. The flow rates of nitrogen and oxygen were controlled by mass
137 flow meters. Good thermal homogeneity along the vertical axis of the JSR was recorded (gradients of < 1 K/cm)
138 by thermocouple measurements (0.1 mm Pt-Pt/Rh-10% wires located inside a thin-wall silica tube). In order to
139 observe the oxidation of these isomers, which are not prone to strong self-ignition, the oxidation of 1% of these
140 chemical compounds ($C_{10}H_{16}$) under lean fuel conditions (equivalence ratio 0.25, 56% O_2 , 43% N_2), experiments
141 were carried out at 590 K, atmospheric pressure, and a residence time of 2 s. Under these conditions, the oxidation
142 of the two isomers is initiated by slow H-atom abstraction by molecular oxygen. The fuel radicals react rapidly
143 with O_2 to form peroxy radicals which undergo further oxidation, characteristic of autoxidation. A 2 mm I.D. probe
144 was used to collect samples. To measure low-temperature oxidation products ranging from early oxidation steps
145 to highly oxidized products, the samples were bubbled into cooled acetonitrile (UHPLC grade ≥ 99.9 , $T = 0^\circ C$, 250
146 mL) for 90 min. The resulting solution was stored in a freezer at $-15^\circ C$. The stability of the products was verified.
147 No detectable changes in the mass spectra were observed after more than one month which is consistent with



5

148 previous findings (Belhadj et al., 2021c). UHPLC conditions were: C₁₈ column and mobile phase containing water-
149 ACN mix at a flow rate of 250 µL/min (gradient 5% to 90% ACN, during 33 min)

150 2.2 Chemical analyses

151 Analyses of samples collected in acetonitrile (ACN) were carried out via direct sample instillation (rate: 3 µL/min
152 and recorded for 1 min for data averaging) in the ionization chamber of a high-resolution mass spectrometer
153 (Thermo Scientific Orbitrap® Q-Exactive, mass resolution 140,000 and mass accuracy <0.5 ppm RMS). Both
154 heated electrospray ionization (HESI) and atmospheric chemical ionization (APCI) were used in positive and
155 negative modes for the ionization of products. HESI settings were: spray voltage 3.8 kV, vaporizer temperature of
156 150°C, capillary temperature 200°C, sheath gas flow of 8 arbitrary units (a.u.), auxiliary gas flow of 1 a.u., sweep
157 gas flow of 0 a.u.. In APCI, settings were: corona discharge current of 3 µA, spray voltage 3.8 kV, vaporizer
158 temperature of 150°C, capillary temperature of 200°C, sheath gas flow of 8 a.u., auxiliary gas flow of 1 a.u., sweep
159 gas flow of 0 a.u.. In order to avoid transmission and detection effects of ions depending on their mass inside the
160 C-Trap (Hecht et al., 2019), acquisitions with three mass ranges were performed (m/z 50-750; m/z 150-750; m/z
161 300-750). The upper limit of m/z 750 was chosen because of the absence of a signal beyond this value. It was
162 shown that no significant oxidation occurred in the HESI and APCI ion sources by injecting a limonene-ACN
163 mixture. The optimization of the Orbitrap ionization parameters in HESI and APCI did not show any clustering
164 phenomenon for these two isomers. The parameters evaluated were: injection source - capillary distance,
165 vaporization and capillary temperatures, applied difference of potential, injected volume, flow rate of nitrogen in
166 the ionization source. Positive and negative HESI mass calibrations were performed using Pierce™ calibration
167 mixtures (Thermo Scientific). Chemical compounds with relative intensity less than 1 ppm to the highest mass
168 peak in the mass spectrum were not considered. Nevertheless, it should be considered that some of the molecules
169 presented in this study could result from our experimental conditions (continuous flow reactor, reagent
170 concentration, temperature, reaction time) and to some extent from our acquisition conditions, different from those
171 in the previous studies (Deng et al., 2021; Quéléver et al., 2019; Meusinger et al., 2017; Krechmer et al., 2016; Tomaz
172 et al., 2021; Fang et al., 2017; Witkowski and Gierczak, 2017; Jokinen et al., 2015; Nørgaard et al., 2013; Bateman
173 et al., 2009; Walser et al., 2008; Warscheid and Hoffmann, 2001; Hammes et al., 2019; Kundu et al., 2012).
174 Operating with continuous flow reactor, elevated temperature, and high initial concentration of reagents allows the
175 formation of combustion-specific products, which does not exclude their possible formation under atmospheric
176 conditions. To assess the formation of products containing OOH and C=O groups, as in previous works (Belhadj
177 et al., 2021a; Belhadj et al., 2021b), H/D exchange with D₂O and 2,4-dinitrophenyl hydrazine derivation were used,
178 respectively

179 3 Data Processing

180 High resolution mass spectrometry (HR-MS) generates large datasets which are difficult to fully analyze by
181 sequential methods. When the study requires the processing of several thousands of molecules, the use of statistical
182 tools and graphical representation means becomes necessary. In this study, we have chosen to use the van Krevelen
183 diagram (Van Krevelen, 1950) by adding an additional dimension, the double bond equivalent (DBE). The DBE
184 number represents the sum of unsaturation and rings present in a chemical compound (Melendez-Perez et al.,



6

185 2016). The interest of this type of representation is to be able to identify more easily the clusters (increase of the
186 DBE number at constant O/C and H/C ratios)

$$187 \quad \text{DBE} = 1 + C - \text{H}/2 - \text{O}$$

188 This number is independent of the number of O-atoms, but changes with the number of hydrogen atoms. Decimal
189 values of this number, which correspond to an odd number of hydrogen atoms, were not considered in this study.
190 Then, duplications of chemical formulas in the O/C vs. H/C space are eliminated. The oxidation state of carbon
191 (OSc) provides a measure of the degree of oxidation of chemical compounds (Kroll et al., 2011). This provides a
192 framework for describing the chemistry of organic species. It is defined by the following equation:

$$193 \quad \text{OSc} \approx 2 \text{O/C} - \text{H/C}$$

194 4 Results and discussion

195 We studied the oxidation of α -pinene and limonene ($\text{C}_{10}\text{H}_{16}$) at 590 K, under atmospheric pressure, with a residence
196 time of 2 s, and a fuel concentration of 1%. Under these conditions, the formation of peroxides by autoxidation at
197 low temperature should be optimal (Belhadj et al., 2021c), even if the conversion of the fuels remains moderate.

198 4.1 Characterization of ionization sources

199 First, we have studied the impact of APCI and HESI sources, in positive and negative modes, on the chemical
200 formulas detected. The HESI and APCI sources in positive and negative mode were used and their operating
201 parameters were varied, i.e., temperature, gas flow and accelerating voltage (see Section 2). For each polarity, only
202 ions composed of carbon, hydrogen (even numbers) and oxygen were considered. Molecular duplicates inherent
203 to mass range overlaps were excluded. Chemical formulas with relative intensity less than 1 ppm with respect to
204 the highest mass peak of the mass spectrum were not considered. By following these rules, we obtained a different
205 number of ions depending on the ionization source and the polarity used. Table 1 shows the number of ions
206 according to the experimental conditions and the discrimination rules.

207 **Table 1.** Number of ions detected for each source in positive and negative modes (by protonation or
208 deprotonation, respectively)

Ionization source	α -Pinene		Limonene	
APCI	646 (R+H) ⁺	503 (R-H) ⁻	1321 (R+H) ⁺	1346 (R-H) ⁻
HESI	594 (R+H) ⁺	693 (R-H) ⁻	1017 (R+H) ⁺	1864 (R-H) ⁻

209

210 Each combination of ionization sources and polarity generated a set of chemical formulas. To make a meaningful
211 comparison between the positive and negative ions data, the chemical formulas used were the precursors of the
212 ions identified in the mass spectra. These sets have common data, but also specific chemical formulas. For a given
213 ionization source, ~ 50% of the chemical formulas are common to both polarities, i.e., between 30 and 50% of
214 molecular species are ignored when using a single polarity (since some of them are ionized under a single mode
215 (+or-) depending on their chemical structure). Then, it is essential to use both polarities in order to better describe



7

216 all the detectable species. The HESI source data were compared to the APCI data (Supplement, Tables S1 and S2),
217 showing an increase of the number of chemical formulas detected by 20 to 30%. This increase is characterized by
218 a better detection of negatively ionized species and those with a higher unsaturation number (DBE). In order to
219 evaluate further the interest for using these ionization sources, we compiled these data in Venn diagrams and
220 proposed a visualization of these sets with a van Krevelen representation; we added the number of DBE in the
221 third dimension (Supplement, Tables S1 and S2).

222 In positive ionization mode, independently of the ionization source and in addition to the common molecular
223 formulas, we detected products with an O/C ratio < 0.2 whereas in the negative ionization mode, we detected
224 molecular formulas with an O/C ratio > 0.5 . In addition to these observations, we noted that HESI is more
225 appropriate for studying products with a large number of unsaturation (DBE > 5), probably related to the increase
226 in the number of hydroxyl groups. Finally, for an optimal detection of the oxidation products, it is necessary to
227 consider the transmission limits of the C-Trap. Here, we could increase by more than 60% the number of molecular
228 formulas detected using several mass ranges for data acquisition (section 2.2). The most appropriate ionization
229 polarity to be used is tight to chemical functions present in products to be detected. We could increase by 30 to
230 100% the number of chemical formulas detected by using both positive and negative ionization modes. Using
231 HESI is consistent with previous findings indicating ESI is well suited for the ionization of acidic, polar, and
232 heteroatom-containing chemicals (Kekäläinen et al., 2013). To illustrate the present results, HESI (-)-MS spectra
233 are provided in the Supplement (Fig. S1).

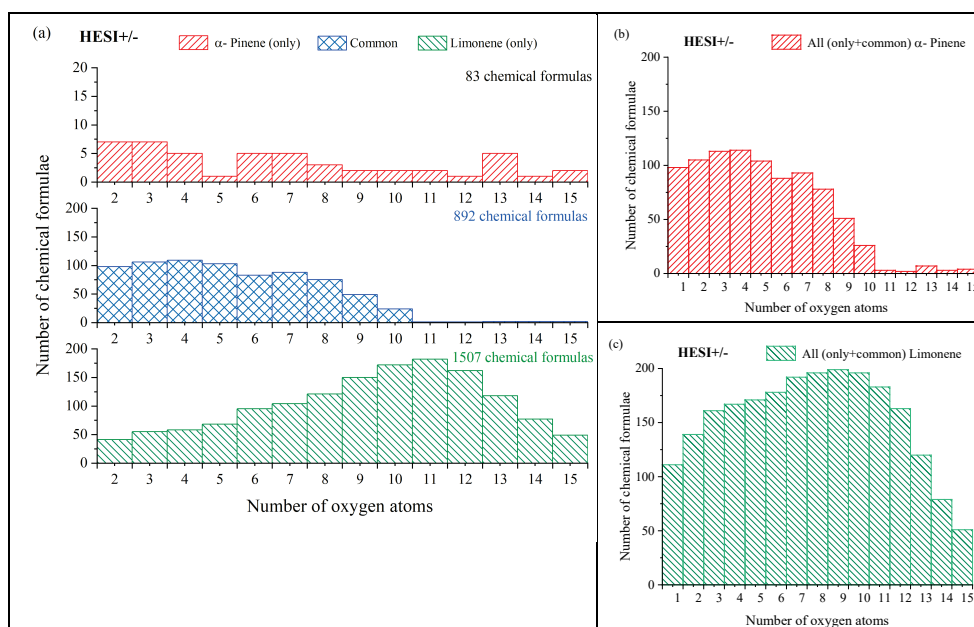
234 *4.2 Autoxidation products detected in a JSR*

235 In order to compare the oxidation of α -pinene and limonene, we compiled the positive and negative ionization data
236 obtained with APCI (Table S1) and HESI (Table S2) ionization sources to obtain a more exhaustive database. For
237 the APCI and HESI sources, we distinguished three datasets, two of which are specific to the oxidation of α -pinene
238 and limonene and one which is common to both isomers. In the following text, "only" will be used to describe the
239 molecules specific to the oxidation of one of the isomeric terpenes. This common dataset represents more than
240 77% of the chemical formulas identified in the α -pinene oxidation samples detected with APCI. For limonene, for
241 which the number of identified chemical formulas is greater, this common dataset represents over 93% of the
242 chemical formulas detected after APCI ionization. In these two cases, the relatively low residence time (2 seconds)
243 and the diversity of the chemical formulas obtained show that the oxidation of these two terpene isomers leads to
244 ring opening, a phenomenon also observed in atmospheric chemistry (Berndt et al., 2016; Zhao et al., 2018; Iyer et
245 al., 2021). Concerning the products molecular formulas common to both isomers, Figure 1 shows that they are
246 limited to 10 oxygen atoms. This limit is linked to α -pinene whose oxidation beyond 10 oxygen atoms remains
247 weak (less than 2% of the totality of the identified molecules for this isomer). In the case of limonene, the presence
248 of an exocyclic double bond will increase, in a similar way to atmospheric chemistry (Kundu et al., 2012), the
249 possibilities of oxidation and accretion. It remains however impossible, considering the size of the whole and the
250 diversity of the isomers, to formalize all the reaction mechanisms. Nevertheless, the formation of oxidized species
251 can be described with the help of graphical tools. The number of oxygen atoms per molecule indicates that
252 limonene oxidizes more than α -pinene (Fig. 1a). In the case of limonene, with a HESI source, an oxygen number
253 of up to 15 is measured, with maximum counts recorded for 10 O-atoms (Fig. 1c), whereas it remains mostly less



8

254 than or equal to 10 for α -pinene (Fig. 1b). Moreover, for the products specific of limonene oxidation, this graph
255 shows a distribution centered on 11 oxygen atoms with carbon skeletons probably resulting from accretion.



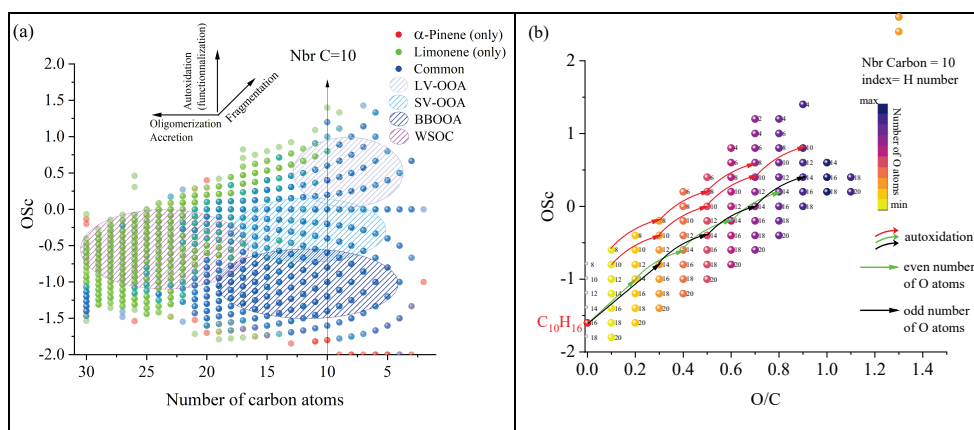
256
257 **Figure 1:** Distribution of α -pinene and limonene autoxidation products as a function of their oxygen content
258 (ionization source: HESI, combined positive and negative modes data). (a) α -pinene and limonene HESI(+/-),
259 (b) α -pinene HESI(+/-), (c) limonene HESI(+/-)

260 To verify this accretion hypothesis, we can plot the OSc as a function of the number of carbon atoms or the O/C
261 ratio at fixed number of C-atoms (Fig. 2). One can visualize the evolution of the molecular oxidation for each
262 carbon skeleton and the formation of oligomers. Species that are unique to one of the isomers, or common to both
263 are differentiated using different colors. In addition to the autoxidation represented by the vertical axis for a given
264 number of carbon atoms (Fig. 2a), we observe mechanisms of fragmentation ($C_{<10}$), accretion and oligomerization
265 ($C_{>10}$). These reaction mechanisms contribute to forming classes according to the size of their carbon skeleton.
266 The increase in the number of oxygen atoms, but also of carbon atoms will decrease products volatility. Following
267 a classification proposed in the literature (Kroll et al., 2011), we distinguished four sets of products: low volatile
268 oxidized organic aerosols (LV-OOA), semi-volatile oxidized organic aerosols (SV-OOA), biomass burning
269 organic aerosols (BBOA) and water-soluble organic carbons (WSOC). The two sets of molecules ionized in APCI
270 and HESI sources (+/-) show that nearly 73% of the molecules are linked to each other by a single difference of 2
271 oxygen atoms, which reflects an autoxidation mechanism. We can measure the extent of autoxidation for each
272 carbon skeleton in the OSc vs. O/C space. For the two terpenes, for which the initial carbon number is equal to 10,
273 one can observe (Fig. 2b) two autoxidation routes with an even and odd number of oxygen atoms, respectively.
274 This parity distinction is initially present for the two main radicals, $ROO\cdot$ and $RO\cdot$, participating to autoxidation.
275 However, termination and propagation reactions will change the oxygen parity. Then, parity links between radicals
276 and molecules are lost, which prevents interpretation of radical oxidation routes (Fig. 3). Figure 2 (b) illustrates

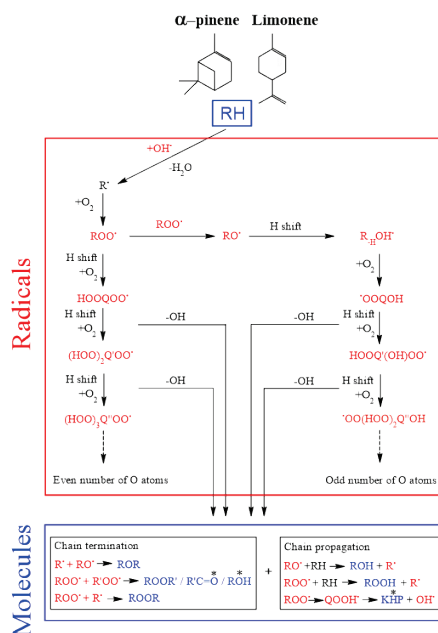


9

277 the autoxidation routes between molecules resulting from a hydroperoxy radical reaction (arrows). In this case the
 278 oxygen parity is not modified and an OH radical is formed. HESI data showed an equivalent distribution of oxygen
 279 parities in molecular products (odd: 51%, even 49%) therefore confirming a lack of selectivity of the reaction
 280 mechanisms with respect to the oxygen parity of radicals.



281 **Figure 2:** Overview of the distribution of limonene and α -pinene oxidation products observed in a JSR: (a) OSc
 282 versus carbon number in detected chemical formulas from APCI and HESI data. (b) OSc versus O/C atomic ratio
 283 for a carbon number of 10; index of the products: number of hydrogen atoms. Arrows indicate autoxidation from
 284 a C₁₀H₁₆ isomer, according to the oxygen parity in products.



285

286 **Figure 3:** Autoxidation radicals reaction mechanisms in combustion (left) and in the atmosphere (left and right).

287 * Indicates a change of oxygen atoms parity.



10

288 **4.3 Combustion versus atmospheric oxidation**

289 *4.3.1 Global analysis*

290 We have explored potential chemical pathways related to autoxidation in the previous Section. For this purpose,
291 we have performed experiments under cool flame conditions (590 K). This autoxidation mechanism is also present
292 in atmospheric chemistry, but it is only recently that it has been found that this mechanism could be one of the
293 main formation pathways for SOA (Savee et al., 2015). Studies have described this mechanism in the case of
294 atmospheric chemistry with the identification of radicals and molecular species (Tomaz et al., 2021). However,
295 previous studies of the propagation of this reaction mechanism mainly focused on the initial skeletons of the C₁₀-
296 terpenes, whereas the other carbon skeletons are also concerned by autoxidation. It is therefore useful to evaluate
297 the proportion of products of autoxidation among the total set chemical species formed.

298 Here, we propose a new approach which consists in assessing a set of molecules mainly resulting from autoxidation
299 against different sets of experimental studies related to atmospheric chemistry. The objective is to evaluate
300 similarity of oxidation products formed under these conditions. For this purpose, we selected a HESI ionization
301 source, better adapted to the polarity of the oxidized molecules, as well as to higher *m/z* (detection of 96% of the
302 total chemical formulas observed in autoxidation by APCI and HESI).

303 Among published atmospheric chemistry studies of terpenes oxidation, we have selected 15 studies presenting
304 enough chemical products of oxidation, 4 for α -pinene and 11 for limonene. The data were acquired using different
305 experimental procedures (methods of oxidation, techniques of characterization). Table 2 summarizes all the
306 experimental parameters related to the selected studies. From that Table, one can note that few studies involved
307 chromatographic analyzes (Tomaz, 2021; Witkowski and Gierczak, 2017; Warscheid and Hoffmann). The data are
308 from the articles or files provided in the Supplement Tables S1 and S2. In these studies, oxidation was performed
309 only by ozonolysis with different experimental conditions that gather the main methods described in the literature:
310 ozonolysis, dark ozonolysis, ozonolysis with OH scavenger, ozonolysis with or without seed particles. We
311 considered that the methods of analysis by mass spectrometry did not modify the nature of the chemical species
312 but only their relative importance, because of the type of ionization and the sensitivity of the instruments. The
313 combination of data obtained using (+/-) HESI gives a rather complete picture of the autoxidation products.

314 First, we compared the data from ozonolysis studies of each terpene and identified similarities through the Venn
315 diagram. For studies with two ionization sources, duplicate chemical formulas were removed. We selected the four
316 most representative studies, by the number of the chemical formulas detected. Then, we compared the set of
317 chemical formulas identified after ozonolysis to those produced in low-temperature combustion, the objective
318 being (i) to highlight similarities in terms of products generated by the two oxidation modes and (ii) to identify
319 chemicals resulting from autoxidation.

320

321



11

322 **Table 2.** Experimental settings of 15 oxidation studies of two terpenes under atmospheric conditions and cool
 323 flames (LC stands for liquid chromatography).

Reference	Oxidation mode	Sampling	Experimental setup	Concentrations of reactants	Ionization /source	Instrument	Chemical formulas	LC
α-Pinene								
Y. Deng et al. (2021)	Dark ozonolysis seed particles OH scavenger	online	Teflon bag; 0.7m ³	3.3±0.6 ncps ppbv ⁻¹ α -Pinene	ESI	ToF-MS	351	No
Quéléver et al. (2019)	Ozonolysis	online	Teflon bag 5 m ³	10 & 50 ppb α -Pinene	NO ₃ ⁻ (CI)	CI-API-TOF	68	No
Meusinger et al. (2017)	Dark Ozonolysis OH scavenger no seed particles	offline	Teflon bag 4.5 m ³	60 ppb α -Pinene	Proton transfer	PTR-MS-ToF	153	No
Krechmer et al. (2016)	Ozonolysis	offline	PAM Oxidation reactor	Field measurement	ESI (-) and NO ₃ ⁻ (CI)	CI-IMS-ToF	43	No
This work	Cool-flame autoxidation	offline	Jet-stirred reactor 42 ml	1%, α -pinene No ozone	APCI(3kV) HESI (3kV)	Orbitrap® Q-Exactive	820 (APCI) 975 (HESI)	Yes
Limonene								
Krechmer et al. (2016)	Ozonolysis	offline	PAM Oxidation reactor	not specified	ESI (-) and NO ₃ ⁻ (CI)	CI-IMS-ToF	63	No
Tomaz et al. (2021)	Ozonolysis	online	Flow tube reactor (18L)	45-227 ppb limonene	NO ₃ ⁻ (CI) - Neg	Orbitrap® Q-Exactive	199	Yes
Fang et al. (2017)	OH-initiated photooxidation dark ozonolysis	online	Smog chamber	900–1500 ppb limonene	UV; 10 eV	Time-of-Flight (ToF)	17	No
Witkowski and Gierczak (2017)	Dark ozonolysis	offline	Flow reactor	2 ppm, limonene	ESI, 4.5 kV	Triple quadrupole	12	Yes
(Jokinen et al., 2015)	Ozonolysis	online	Flow glass tube	1–10000 x10 ⁹ molec.cm ⁻³ , limonene	chemical ionization	Time-of-Flight (ToF)	11	No
Nørgaard et al. (2013)	Ozone (plasma)	online	direct on the support	850 ppb ozone 15-150 ppb limonene	plasma	Quadrupole time-of-flight (QToF)	29	No
Bateman et al. (2009)	Dark and UV radiations ozonolysis	offline	Teflon FEP reaction chamber	1 ppm ozone 1 ppm limonene	modified ESI (+/-)	LTQ-Orbitrap Hybrid Mass (ESI)	924	No
Walser et al. (2008)	Dark ozonolysis	offline	Teflon FEP reaction chamber	1-10 ppm ozone 10 ppm limonene	ESI (+/-); 4.5 kV	LTQ-Orbitrap Hybrid Mass (ESI)	465	No
Warscheid & Hoffmann (2001)	Ozonolysis	online	Smog chamber	300-500 ppb limonene	APCI; 3kV	Quadrupole ion trap mass	21	Yes
Hammes et al., (2019)	Dark ozonolysis	online	Flow reactor	15, 40, 150 ppb limonene	²¹⁰ Po α -	HR-ToF-CIMS	20	No
Kundu et al. (2012)	Dark ozonolysis	offline	Teflon reaction chamber	250 ppb ozone 500 ppb limonene	ESI; 3.7 and 4 kV	LTQ FT Ultra, Thermo Sct (ESI)	1197	No
This work	Cool-flame autoxidation	offline	Jet-stirred reactor 42 ml	1%, limonene No ozone	APCI(3 μ A) HESI (3kV)	Orbitrap® Q-Exactive	1863(APCI) 2399(HESI)	Yes

324

325 For α -pinene oxidation, the four selected studies 567 chemical formulas were detected, all polarities combined.

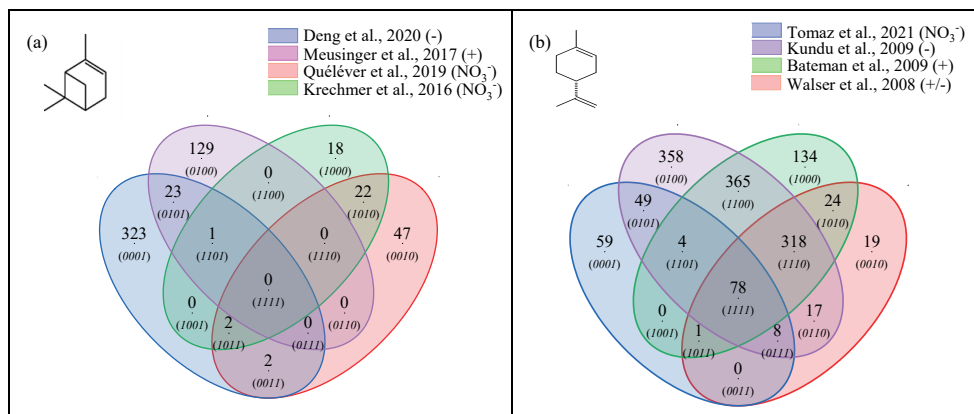
326 Only one study (Meusinger et al., 2017) was performed in positive mode and none of the studies reported data



12

327 were obtained with two ionization modes (+/-). For limonene oxidation, the four studies selected identified 1434
328 chemical formulas. Only one study (Walser et al., 2008) used (+) and (-) ionization modes. In the case of limonene
329 oxidation, for which accretion is more important than for α -pinene, and for which a greater number of chemical
330 formulas were identified, the similarities are more important. These results are presented in Figure 4 where the
331 ionization polarity used in each study is specified.

332



333 **Figure 4:** Venn diagrams for comparing the oxidation results from ozonolysis of (a) α -pinene and (b) limonene
334 (see conditions in Table 1). Each digit of the binary numbers in parentheses identifies the datasets being
335 compared.

336 For α -pinene, no chemical formula is common to all datasets. Different hypotheses can be offered to explain this
337 result. Among them, the number of chemical formulas identified per study remains limited (a few dozen to several
338 hundred) and these small datasets are sometimes restricted to specific mass ranges, e.g. C_{10} to C_{20} (Quéléver et al.,
339 2019). In the case of studies carried out with an NO_3^- source, sensitive to HOMS, produced preferentially by
340 autoxidation, we note that nearly 50% of the chemical formulas (10/22; (1010)) are linked by a simple difference
341 of 2 oxygen atoms.

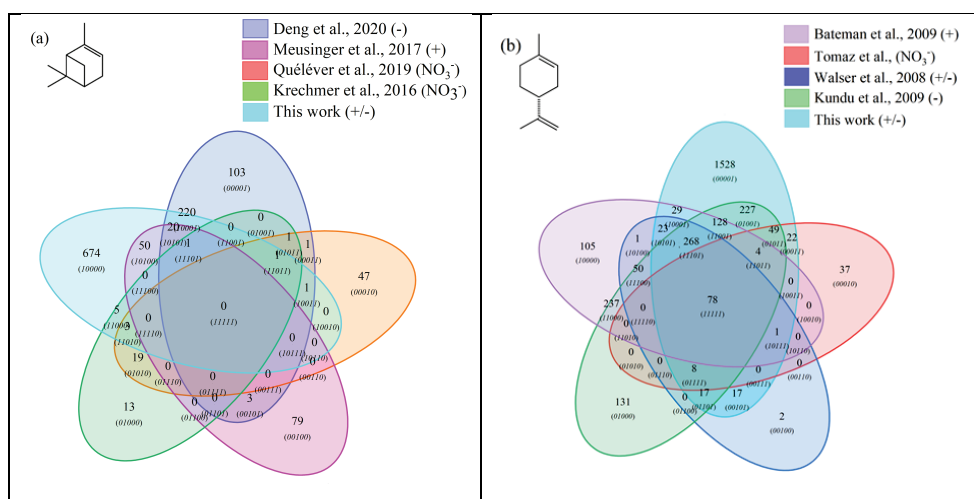
342 For limonene, 78 chemical formulas are common to the four studies selected here. In this data set, a large majority
343 of chemical formulas show a similar relationship to autoxidation: 62% (Tomaz et al., 2021), 54% (Walser et al.,
344 2008), 69% (Kundu et al., 2012), 66% (Bateman et al., 2009) and 72% (this study), simple difference of two
345 oxygen atoms). This result seems to indicate that autoxidation dominates.

346 One can then ask if reaction mechanisms common to atmospheric and combustion chemistry can generate, despite
347 radically different experimental conditions, a set of common chemical formulas and if in this common dataset, a
348 common link, characteristic of autoxidation, is observable? To address that question, we compared all the previous
349 results, for each of these terpenes to those obtained under the present combustion study. The comparisons were
350 made using HESI data. One should remember that the oxidation conditions in a JSR were chosen in order to
351 maximize low-temperature autoxidation. Again, we used Venn diagrams to analyze these datasets composed of
352 1590 chemical formulas in the case of α -pinene and 5184 chemical formulas in the case of limonene. The results
353 of these analyses are presented in Figure 5.



13

354 It turned out that for α -pinene, 301 chemical formulas and for limonene 871 chemical formulas were common to
355 oxidation by ozonolysis and combustion. This represents 31% of the chemical formulas for the ozonolysis of α -
356 pinene and 36% for those of limonene ozonolysis. For α -pinene, the similarities compared to combustion are
357 specific to each study: (Deng et al., 2021) 69%, (Meusinger et al., 2017) 46%, (Quéléver et al., 2019) 7%,
358 (Krechmer et al., 2016) 23%. Chemical formulas common to all studies were not identified. This lack of similarity
359 may be due to a partial characterization of the chemical formulas, a weaker oxidation of α -pinene with an ionization
360 mode less favorable to low molecular weights.

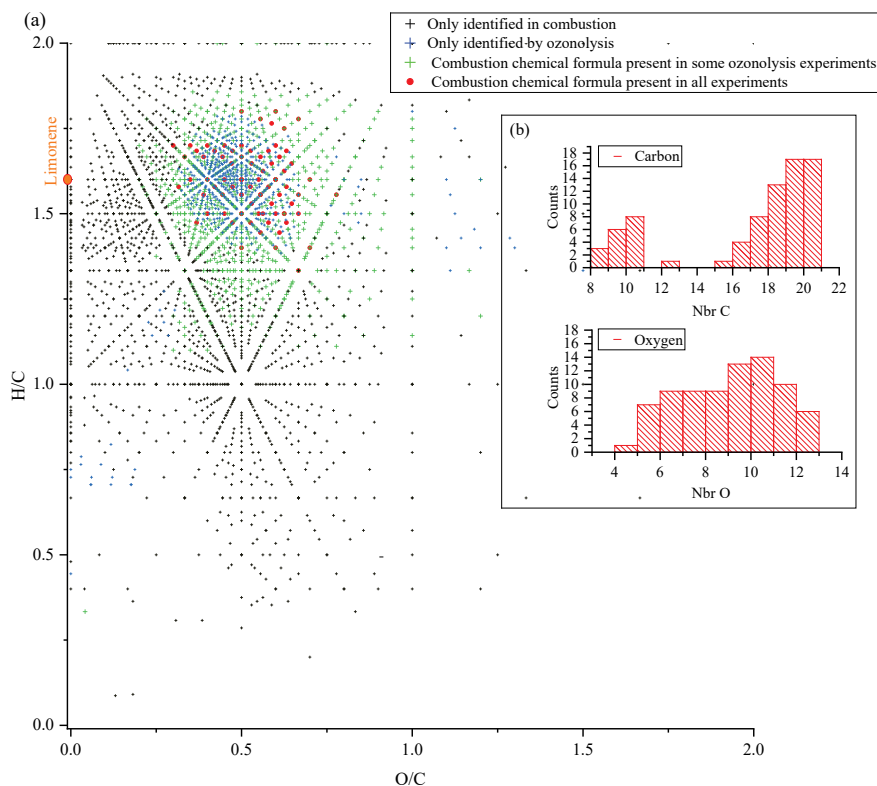


361 **Figure 5:** Venn diagrams comparing the oxidation results from ozonolysis and combustion of (a) α -pinene and
362 (b) limonene (see conditions in Table 1).

363 For limonene, the similarities with combustion are more important and less spread out. They represent for the
364 different studies: 65% (Kundu et al., 2012), 88% (Walser et al., 2008), 81% (Tomaz et al., 2021), 57% (Bateman
365 et al., 2009). Moreover, there is a common dataset of 78 chemical formulas which can derive from autoxidation
366 mechanisms. It is necessary to specify again that different reaction mechanisms can cause the observed similarities.
367 However, the preponderance of autoxidation in so-called cool flame combustion is obvious, and in atmospheric
368 chemistry, this reaction mechanism is competitive or dominates (Crouse et al., 2013; Jokinen et al., 2014). If we
369 search for an autoxidation link between these 78 chemical formulas, we observe that 45% of these chemical
370 formulas meet this condition: difference of two oxygen atoms between formulas, at constant number of carbon
371 and hydrogen atoms. More precisely, these molecules are centered in a van Krevelen diagram on the ratios $O/C=0.6$
372 and $H/C=1.6$, in the range $0.29 < O/C < 0.77$ and $1.33 < H/C < 1.8$. All oxidized molecules associated with this
373 dataset are presented in Figure 6. The dispersion of the chemical formulas, far from being random, remains
374 consistent with an autoxidation mechanism where the numbers of carbon and hydrogen atoms are constant.



14



375

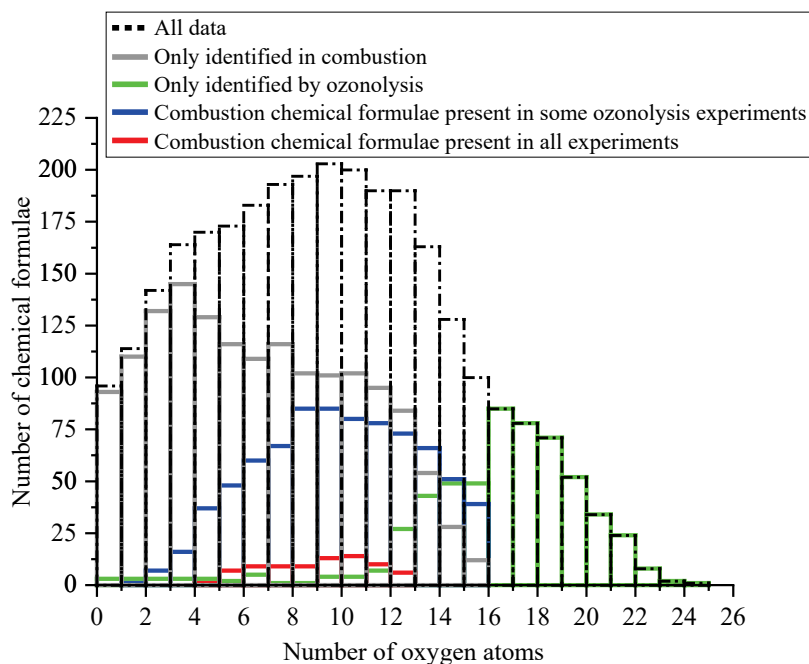
376 **Figure 6:** (a) Van Krevelen diagram showing specific and common chemical formulas detected after to
377 oxidation of limonene by ozonolysis and combustion, insert (b): distributions of the number of carbon and
378 oxygen atoms in the 78 chemical formulas common to all experiments.

379 A 3-D representation of all limonene oxidation data is given in Supplement (Fig. S2) where DBE is used as third
380 dimension. From that figure, one can note that products with higher DBE ($DBE > 10$) are preferably formed under
381 JSR conditions, i.e. at elevated temperature. The corresponding chemical formulas could correspond to carbonyls
382 and / or cyclic ethers ($^{\cdot}QOOH \rightarrow \text{carbonyl} + \text{alkene} + \text{OH}$ and / or cyclic ether + OH). Specificities and similarities
383 of these two oxidation modes (ozonolysis/combustion) were further investigated by plotting the distribution of the
384 number of oxygen atoms in detected chemical formulas (Fig. 7). Indeed, the distribution of the number of oxygen
385 atoms allows, in addition to the Van Krevelen diagram, to provide some additional details on these two modes of
386 oxidation. In ozonolysis, we observed the chemical formulas having the largest number of oxygen atoms. There,
387 oxidation proceeds over a long reaction time where the phenomenon of aging appears by promoting accretion or
388 oligomerization. In combustion, the number of oxygen atoms remains limited to 18, with a lower number of
389 detected chemical formulas compared to the case of ozonolysis. However, it is in combustion that we observed the
390 highest O/C ratios, indicating the formation of the most oxidized products. This difference, however, does not
391 affect the similarities between the chemical formulas detected in the two modes of oxidation. Finally, the analysis
392 of the parities in oxygen atoms, very similar for the three datasets, confirms that the reaction mechanisms presented



15

393 in Figure 3 do not allow a simple link to be established between the oxygen parity of radicals and that of molecular
394 products.



395
396 **Figure 7:** Oxygen number distribution for all the molecules identified for the oxidation of limonene: only in
397 combustion, only in ozonolysis and common to both processes.

398 4.3.2 Detailed analysis

399 UHPLC analyzes were carried out in order to characterize isomers in combustion products and their possible
400 similarities with those detected in atmospheric chemistry. We have targeted chemical formulas common to
401 atmospheric and combustion chemistry, corresponding to the first stages of oxidation: $C_{10}H_{16}O_2$ (10101) and
402 $C_{10}H_{16}O_3$ (11101), in order to limit the number of isomers. In the literature, UHPLC data on these two chemical
403 formulas remain limited both in atmospheric and in combustion (Table 2, LC column). Nevertheless, in
404 atmospheric chemistry, different isomers have been identified for these two chemical formulas. Table 3 presents
405 these isomers for α -pinene and limonene, together with bibliographic references.

406 The UHPLC analyzes of combustion derived samples showed the presence of several isomers, inevitably coeluted.
407 Here, we have detected the presence of -OH or -OOH and C=O groups through H/D exchange with D_2O and
408 derivatization of carbonyls with 2,4-DNPH, respectively. Our results are presented in Fig. 8. They show the
409 presence of several -OH and carbonyl groups. Furthermore, we verified that the main isomers identified in
410 atmospheric chemistry were present (i.e. $C_{10}H_{16}O_5$ (11111), $C_{10}H_{16}O_7$ (11111), $C_{10}H_{16}O_9$ (01011), $C_{10}H_{14}O_8$
411 (01011)), and compatible with an autoxidation reaction mechanism (Fig S3). Unfortunately, coelution did not fully
412 allow exploiting MS/MS fragmentation carried out on the two chemical formulas, and to formally identify the
413 isomers.

414

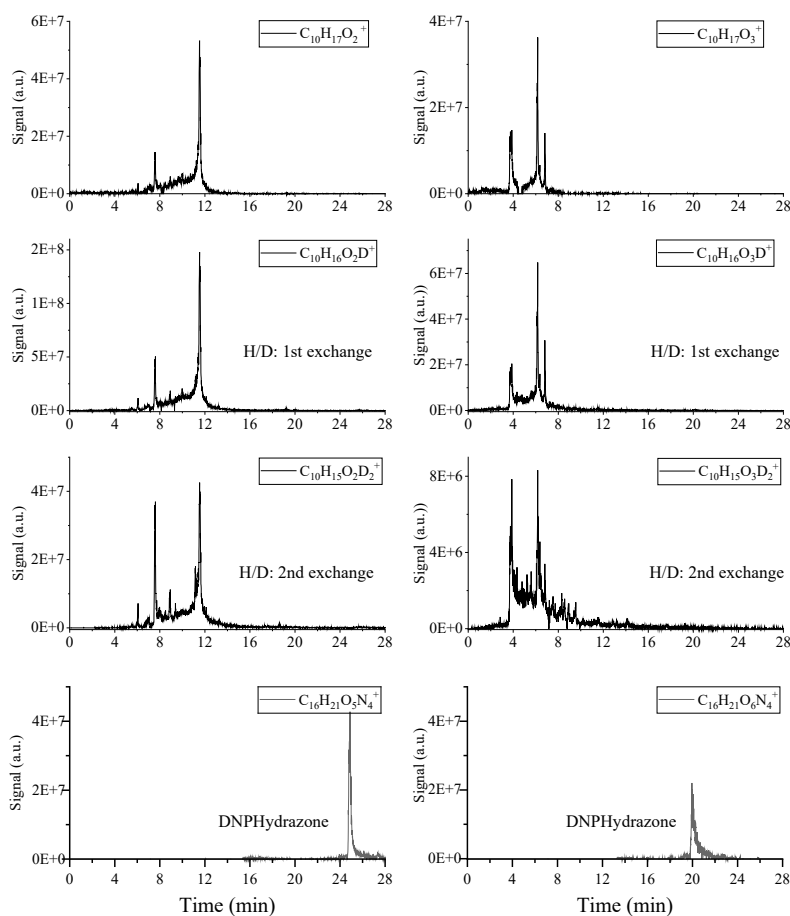


16

415 **Table 3.** Isomers of α -pinene and limonene oxidation reported in the literature.

	$C_{10}H_{16}O_2$		$C_{10}H_{16}O_3$	
α -pinene	Pinonaldehyde	(Fang et al., 2017)	Pinonic acid	(Fang et al., 2017; Ng et al., 2011; Meusinger et al., 2017)
	hydroxyketone	(Fang et al., 2017)	hydroxy pinonaldehydes	(Fang et al., 2017; Meusinger et al., 2017)
Limonene	limononaldehyde	(Fang et al., 2017; Walser et al., 2008; Bateman et al., 2009)	limononic acid	(Fang et al., 2017; Witkowski and Gierczak, 2017; Hammes et al., 2019; Walser et al., 2008; Bateman et al., 2009; Warscheid and Hoffmann, 2001)
	4-isopropenyl-methylhydroxy-2-oxocyclohexane	(Fang et al., 2017)	7-hydroxy-limononaldehyde	(Fang et al., 2017; Walser et al., 2008; Bateman et al., 2009; Meusinger et al., 2017)

416



417

418 **Fig 8:** Left, $C_{10}H_{16}O_2$ chromatogram with D_2O exchange and DNPH derivatization. Right, $C_{10}H_{16}O_3$
 419 chromatogram with D_2O exchange and DNPH derivatization. One should note that no deuterated chemicals
 420 could be detected before addition of D_2O .



17

421 5 Conclusion

422 The oxidation of limonene-oxygen-nitrogen and α -pinene-oxygen-nitrogen mixtures was carried out using a jet-
423 stirred reactor at elevated temperature (590 K), a residence time of 2 s, and atmospheric pressure. The products
424 were analyzed by liquid chromatography, flow injection, and soft ionization-high resolution mass spectrometry.
425 H/D exchange and 2,4-dinitrophenyl hydrazine derivatization were used to assess the presence of OOH and C=O
426 groups in products, respectively. We probed the effects of the type of ionization used in mass spectrometry analyses
427 on the detection of oxidation products. Heated electrospray ionization (HESI +/-) and atmospheric pressure
428 chemical ionization (APCI +/-) were used. A large dataset was obtained and compared with literature data obtained
429 during the oxidation of limonene and α -pinene under simulated tropospheric and low-temperature oxidation
430 conditions. This work showed a surprisingly similar set of chemical formulas of products, including oligomers,
431 formed under the two rather different conditions, i.e., cool flames and simulated atmospheric oxidation. Data
432 analysis involving van Krevelen diagrams, oxygen number distribution, oxidation state of carbon, and chemical
433 relationship between molecules, indicated that a subset of chemical formulas is common to all experiments
434 independently of experimental conditions. More than 35% of the chemical formulas detected in combustion
435 chemistry experiments using a JSR have been detected in the studies carried out under atmospheric conditions.
436 Finally, we have outlined the existence of a substantial common dataset of autoxidation products. This result tends
437 to show that autoxidation is indeed inducing similarity between atmospheric and combustion products. Detailed
438 analysis of our data was performed by UHPLC-MS/MS of selected chemical formulas observed in the literature.
439 Nevertheless, final identification was not possible due to coelutions.

440 The present JSR data could be useful to atmospheric chemists working in the field of wildfire and/or biomass
441 burning induced air pollution. Considering that low-temperature oxidation (cool flame) products, i.e., COVs, can
442 be emitted from biomass burning, wildfires and engine exhausts, the present data should be of interest for the
443 atmospheric chemists because they complement those obtained in atmospheric chemistry literature. It would be
444 interesting to complement the atmospheric relevant data with MS² analyses of products and assessment of the
445 presence of hydroperoxyl and carbonyl groups HOMs. Further MS² characterizations are also needed for the
446 products observed in the present work. Finally, a study of the temperature dependence of products formation would
447 be very useful, both under cool flame conditions and simulated atmospheric oxidation conditions.

448

449 Acknowledgements

450 The authors gratefully acknowledge funding from the Labex Caprysses (ANR-11-LABX-0006-01), the Labex
451 Voltaire (ANR-10-LABX-100-01), CPER, and EFRD (PROMESTOCK and APPROPOR-e projects) and the
452 French MESRI for a Ph.D. grant. We also thank Matthieu Riva for sharing his experimental data on limonene
453 oxidation.

454

455

456



18

457 References

- 458 Bailey, H. C., and Norrish, R. G. W.: The oxidation of hexane in the cool-flame region, Proceedings of
459 the Royal Society of London Series a-Mathematical and Physical Sciences, 212, 311-330,
460 10.1098/rspa.1952.0084, 1952.
- 461 Bateman, A. P., Nizkorodov, S. A., Laskin, J., and Laskin, A.: Time-resolved molecular characterization
462 of limonene/ozone aerosol using high-resolution electrospray ionization mass spectrometry,
463 Physical Chemistry Chemical Physics, 11, 7931-7942, 10.1039/B905288G, 2009.
- 464 Belhadj, N., Benoit, R., Dagaut, P., Lailliau, M., Serinyel, Z., Dayma, G., Khaled, F., Moreau, B., and
465 Foucher, F.: Oxidation of di-n-butyl ether: Experimental characterization of low-temperature
466 products in JSR and RCM, Combustion and Flame, 222, 133-144,
467 /10.1016/j.combustflame.2020.08.037, 2020.
- 468 Belhadj, N., Benoit, R., Dagaut, P., and Lailliau, M.: Experimental characterization of n-heptane low-
469 temperature oxidation products including keto-hydroperoxides and highly oxygenated organic
470 molecules (HOMs), Combustion and Flame, 224, 83-93, /10.1016/j.combustflame.2020.10.021,
471 2021a.
- 472 Belhadj, N., Lailliau, M., Benoit, R., and Dagaut, P.: Towards a Comprehensive Characterization of the
473 Low-Temperature Autoxidation of Di-n-Butyl Ether, Molecules, 26, 7174, 2021b.
- 474 Belhadj, N., Lailliau, M., Benoit, R., and Dagaut, P.: Experimental and kinetic modeling study of n-
475 hexane oxidation. Detection of complex low-temperature products using high-resolution mass
476 spectrometry, Combustion and Flame, 233, 111581, /10.1016/j.combustflame.2021.111581,
477 2021c.
- 478 Benoit, R., Belhadj, N., Lailliau, M., and Dagaut, P.: On the similarities and differences between the
479 products of oxidation of hydrocarbons under simulated atmospheric conditions and cool
480 flames, Atmos. Chem. Phys., 21, 7845-7862, 10.5194/acp-21-7845-2021, 2021.
- 481 Benson, S. W.: The kinetics and thermochemistry of chemical oxidation with application to
482 combustion and flames, Progress in Energy and Combustion Science, 7, 125-134,
483 /10.1016/0360-1285(81)90007-1, 1981.
- 484 Bernath, P., Boone, C., and Crouse, J.: Wildfire smoke destroys stratospheric ozone, Science, 375,
485 1292-1295, doi:10.1126/science.abm5611, 2022.
- 486 Berndt, T., Richters, S., Kaethner, R., Voigtländer, J., Stratmann, F., Sipilä, M., Kulmala, M., and
487 Herrmann, H.: Gas-Phase Ozonolysis of Cycloalkenes: Formation of Highly Oxidized RO₂
488 Radicals and Their Reactions with NO, NO₂, SO₂, and Other RO₂ Radicals, The Journal of
489 Physical Chemistry A, 119, 10336-10348, 10.1021/acs.jpca.5b07295, 2015.
- 490 Berndt, T., Richters, S., Jokinen, T., Hyttinen, N., Kurtén, T., Otkjær, R. V., Kjaergaard, H. G.,
491 Stratmann, F., Herrmann, H., Sipilä, M., Kulmala, M., and Ehn, M.: Hydroxyl radical-induced
492 formation of highly oxidized organic compounds, Nature Communications, 7, 13677,
493 10.1038/ncomms13677, 2016.
- 494 Bianchi, F., Kurtén, T., Riva, M., Mohr, C., Rissanen, M. P., Roldin, P., Berndt, T., Crouse, J. D.,
495 Wennberg, P. O., Mentel, T. F., Wildt, J., Junninen, H., Jokinen, T., Kulmala, M., Worsnop, D. R.,
496 Thornton, J. A., Donahue, N., Kjaergaard, H. G., and Ehn, M.: Highly Oxygenated Organic
497 Molecules (HOM) from Gas-Phase Autoxidation Involving Peroxy Radicals: A Key Contributor to
498 Atmospheric Aerosol, Chemical Reviews, 119, 3472-3509, 10.1021/acs.chemrev.8b00395,
499 2019.
- 500 Cox, R. A., and Cole, J. A.: Chemical aspects of the autoignition of hydrocarbon-air mixtures, Combust.
501 Flame, 60, 109-123, /10.1016/0010-2180(85)90001-X, 1985.
- 502 Crouse, J. D., Nielsen, L. B., Jørgensen, S., Kjaergaard, H. G., and Wennberg, P. O.: Autoxidation of
503 organic compounds in the atmosphere, J. Phys. Chem. Lett., 4, 3513, 10.1021/jz4019207, 2013.
- 504 Dagaut, P., Cathonnet, M., Rouan, J. P., Foulatier, R., Quilgars, A., Boettner, J. C., Gaillard, F., and
505 James, H.: A jet-stirred reactor for kinetic studies of homogeneous gas-phase reactions at
506 pressures up to ten atmospheres (≈ 1 MPa), Journal of Physics E: Scientific Instruments, 19, 207-
507 209, 10.1088/0022-3735/19/3/009, 1986.



19

- 508 Dagaut, P., Cathonnet, M., Boetner, J. C., and Gaillard, F.: Kinetic Modeling of Propane Oxidation,
509 Combustion Science and Technology, 56, 23-63, 10.1080/00102208708947080, 1987.
- 510 Dagaut, P., Cathonnet, M., Boettner, J. C., and Gaillard, F.: Kinetic modeling of ethylene oxidation,
511 Combustion and Flame, 71, 295-312, /10.1016/0010-2180(88)90065-X, 1988.
- 512 Deng, Y., Inomata, S., Sato, K., Ramasamy, S., Morino, Y., Enami, S., and Tanimoto, H.: Temperature
513 and acidity dependence of secondary organic aerosol formation from α -pinene ozonolysis with
514 a compact chamber system, Atmos. Chem. Phys., 21, 5983-6003, 10.5194/acp-21-5983-2021,
515 2021.
- 516 Fang, W., Gong, L., and Sheng, L.: Online analysis of secondary organic aerosols from OH-initiated
517 photooxidation and ozonolysis of α -pinene, β -pinene, Δ^3 -carene and d-limonene by thermal
518 desorption-photoionisation aerosol mass spectrometry, Environmental Chemistry, 14, 75-90,
519 /10.1071/EN16128, 2017.
- 520 Gilman, J. B., Lerner, B. M., Kuster, W. C., Goldan, P. D., Warneke, C., Veres, P. R., Roberts, J. M., de
521 Gouw, J. A., Burling, I. R., and Yokelson, R. J.: Biomass burning emissions and potential air
522 quality impacts of volatile organic compounds and other trace gases from fuels common in the
523 US, Atmos. Chem. Phys., 15, 13915-13938, 10.5194/acp-15-13915-2015, 2015.
- 524 Hammes, J., Lutz, A., Mentel, T., Faxon, C., and Hallquist, M.: Carboxylic acids from limonene
525 oxidation by ozone and hydroxyl radicals: insights into mechanisms derived using a S4AERO-
526 CIMS, Atmos. Chem. Phys., 19, 13037-13052, 10.5194/acp-19-13037-2019, 2019.
- 527 Harvey, B. G., Wright, M. E., and Quintana, R. L.: High-Density Renewable Fuels Based on the
528 Selective Dimerization of Pinenes, Energy Fuels, 24, 267-273, 10.1021/ef900799c, 2010.
- 529 Harvey, B. G., Merriman, W. W., and Koontz, T. A.: High-Density Renewable Diesel and Jet Fuels
530 Prepared from Multicyclic Sesquiterpanes and a 1-Hexene-Derived Synthetic Paraffinic
531 Kerosene, Energy Fuels, 29, 2431-2436, 10.1021/ef5027746, 2015.
- 532 Hatch, L. E., Jen, C. N., Kreisberg, N. M., Selimovic, V., Yokelson, R. J., Stamatis, C., York, R. A., Foster,
533 D., Stephens, S. L., Goldstein, A. H., and Barsanti, K. C.: Highly Speciated Measurements of
534 Terpenoids Emitted from Laboratory and Mixed-Conifer Forest Prescribed Fires, Environmental
535 Science & Technology, 53, 9418-9428, 10.1021/acs.est.9b02612, 2019.
- 536 Hecht, E. S., Scigelova, M., Eliuk, S., and Makarov, A.: Fundamentals and Advances of Orbitrap Mass
537 Spectrometry, Encyclopedia of Analytical Chemistry, 1-40,
538 10.1002/9780470027318.a9309.pub2, 2019.
- 539 Huang, W., Saathoff, H., Pajunoja, A., Shen, X., Naumann, K. H., Wagner, R., Virtanen, A., Leisner, T.,
540 and Mohr, C.: α -Pinene secondary organic aerosol at low temperature: chemical composition
541 and implications for particle viscosity, Atmos. Chem. Phys., 18, 2883-2898, 10.5194/acp-18-
542 2883-2018, 2018.
- 543 Iyer, S., Rissanen, M. P., Valiev, R., Barua, S., Krechmer, J. E., Thornton, J., Ehn, M., and Kurtén, T.:
544 Molecular mechanism for rapid autoxidation in α -pinene ozonolysis, Nature Communications,
545 12, 878, 10.1038/s41467-021-21172-w, 2021.
- 546 Jokinen, T., Sipilä, M., Richters, S., Kerminen, V.-M., Paasonen, P., Stratmann, F., Worsnop, D.,
547 Kulmala, M., Ehn, M., Herrmann, H., and Berndt, T.: Rapid Autoxidation Forms Highly Oxidized
548 RO₂ Radicals in the Atmosphere, Angewandte Chemie International Edition, 53, 14596-14600,
549 /10.1002/anie.201408566, 2014.
- 550 Jokinen, T., Berndt, T., Makkonen, R., Kerminen, V.-M., Junninen, H., Paasonen, P., Stratmann, F.,
551 Herrmann, H., Guenther, A. B., Worsnop, D. R., Kulmala, M., Ehn, M., and Sipilä, M.: Production
552 of extremely low volatile organic compounds from biogenic emissions: Measured yields and
553 atmospheric implications, Proceedings of the National Academy of Sciences, 112, 7123,
554 10.1073/pnas.1423977112, 2015.
- 555 Kekäläinen, T., Pakarinen, J. M. H., Wickström, K., Lobodin, V. V., McKenna, A. M., and Jänis, J.:
556 Compositional Analysis of Oil Residues by Ultrahigh-Resolution Fourier Transform Ion Cyclotron
557 Resonance Mass Spectrometry, Energy Fuels, 27, 2002-2009, 10.1021/ef301762v, 2013.
- 558 Khaykin, S., Legras, B., Bucci, S., Sellitto, P., Isaksen, I., Tencé, F., Bekki, S., Bourassa, A., Rieger, L.,
559 Zawada, D., Jumelet, J., and Godin-Beekmann, S.: The 2019/20 Australian wildfires generated a



20

- 560 persistent smoke-charged vortex rising up to 35 km altitude, *Communications Earth &*
561 *Environment*, 1, 22, 10.1038/s43247-020-00022-5, 2020.
- 562 Kobziar, L. N., Pingree, M. R. A., Larson, H., Dreaden, T. J., Green, S., and Smith, J. A.:
563 Pyroaerobiology: the aerosolization and transport of viable microbial life by wildland fire,
564 *Ecosphere*, 9, e02507, /10.1002/ecs2.2507, 2018.
- 565 Korcek, S., Ingold, K. U., Chenier, J. H. B., and Howard, J. A.: Absolute rate constants for hydrocarbon
566 autoxidation .21. Activation-energies for propagation and correlation of propagation rate
567 constants with carbon-hydrogen bond strengths, *Canadian Journal of Chemistry*, 50, 2285-&
568 10.1139/v72-365, 1972.
- 569 Kourtchev, I., Doussin, J. F., Giorio, C., Mahon, B., Wilson, E. M., Maurin, N., Pangui, E., Venables, D.
570 S., Wenger, J. C., and Kalberer, M.: Molecular composition of fresh and aged secondary organic
571 aerosol from a mixture of biogenic volatile compounds: a high-resolution mass spectrometry
572 study, *Atmos. Chem. Phys.*, 15, 5683-5695, 10.5194/acp-15-5683-2015, 2015.
- 573 Krechmer, J. E., Groessl, M., Zhang, X., Junninen, H., Massoli, P., Lambe, A. T., Kimmel, J. R., Cubison,
574 M. J., Graf, S., Lin, Y. H., Budisulistiorini, S. H., Zhang, H., Surratt, J. D., Knochenmuss, R., Jayne,
575 J. T., Worsnop, D. R., Jimenez, J. L., and Canagaratna, M. R.: Ion mobility spectrometry–mass
576 spectrometry (IMS–MS) for on- and offline analysis of atmospheric gas and aerosol species,
577 *Atmos. Meas. Tech.*, 9, 3245-3262, 10.5194/amt-9-3245-2016, 2016.
- 578 Kristensen, K., Watne, Å. K., Hammes, J., Lutz, A., Petäjä, T., Hallquist, M., Bilde, M., and Glasius, M.:
579 High-Molecular Weight Dimer Esters Are Major Products in Aerosols from α -Pinene Ozonolysis
580 and the Boreal Forest, *Environmental Science & Technology Letters*, 3, 280-285,
581 10.1021/acs.estlett.6b00152, 2016.
- 582 Kroll, J. H., Donahue, N. M., Jimenez, J. L., Kessler, S. H., Canagaratna, M. R., Wilson, K. R., Altieri, K.
583 E., Mazzoleni, L. R., Wozniak, A. S., Bluhm, H., Mysak, E. R., Smith, J. D., Kolb, C. E., and
584 Worsnop, D. R.: Carbon oxidation state as a metric for describing the chemistry of atmospheric
585 organic aerosol, *Nature Chemistry*, 3, 133-139, 10.1038/nchem.948, 2011.
- 586 Kundu, S., Fisseha, R., Putman, A. L., Rahn, T. A., and Mazzoleni, L. R.: High molecular weight SOA
587 formation during limonene ozonolysis: insights from ultrahigh-resolution FT-ICR mass
588 spectrometry characterization, *Atmos. Chem. Phys.*, 12, 5523-5536, 10.5194/acp-12-5523-
589 2012, 2012.
- 590 Kurtén, T., Rissanen, M. P., Mackeprang, K., Thornton, J. A., Hyttinen, N., Jørgensen, S., Ehn, M., and
591 Kjaergaard, H. G.: Computational Study of Hydrogen Shifts and Ring-Opening Mechanisms in α -
592 Pinene Ozonolysis Products, *The Journal of Physical Chemistry A*, 119, 11366-11375,
593 10.1021/acs.jpca.5b08948, 2015.
- 594 Melendez-Perez, J. J., Martínez-Mejía, M. J., and Eberlin, M. N.: A reformulated aromaticity index
595 equation under consideration for non-aromatic and non-condensed aromatic cyclic carbonyl
596 compounds, *Organic Geochemistry*, 95, 29-33, /10.1016/j.orggeochem.2016.02.002, 2016.
- 597 Meusinger, C., Dusek, U., King, S. M., Holzinger, R., Rosenørn, T., Sperlich, P., Julien, M., Remaud, G.
598 S., Bilde, M., Röckmann, T., and Johnson, M. S.: Chemical and isotopic composition of
599 secondary organic aerosol generated by α -pinene ozonolysis, *Atmos. Chem. Phys.*, 17, 6373-
600 6391, 10.5194/acp-17-6373-2017, 2017.
- 601 Mewalal, R., Rai, D. K., Kainer, D., Chen, F., Külheim, C., Peter, G. F., and Tuskan, G. A.: Plant-Derived
602 Terpenes: A Feedstock for Specialty Biofuels, *Trends Biotechnol.*, 35, 227-240,
603 /10.1016/j.tibtech.2016.08.003, 2017.
- 604 Ng, N. L., Canagaratna, M. R., Jimenez, J. L., Chhabra, P. S., Seinfeld, J. H., and Worsnop, D. R.:
605 Changes in organic aerosol composition with aging inferred from aerosol mass spectra, *Atmos.*
606 *Chem. Phys.*, 11, 6465-6474, 10.5194/acp-11-6465-2011, 2011.
- 607 Nørgaard, A. W., Vibenholt, A., Benassi, M., Clausen, P. A., and Wolkoff, P.: Study of Ozone-Initiated
608 Limonene Reaction Products by Low Temperature Plasma Ionization Mass Spectrometry,
609 *Journal of The American Society for Mass Spectrometry*, 24, 1090-1096, 10.1007/s13361-013-
610 0648-3, 2013.



21

- 611 Nozière, B., Kalberer, M., Claeys, M., Allan, J., D'Anna, B., Decesari, S., Finessi, E., Glasius, M., Grgić, I.,
612 Hamilton, J. F., Hoffmann, T., Iinuma, Y., Jaoui, M., Kahnt, A., Kampf, C. J., Kourtchev, I.,
613 Maenhaut, W., Marsden, N., Saarikoski, S., Schnelle-Kreis, J., Surratt, J. D., Szidat, S.,
614 Szmigielski, R., and Wisthaler, A.: The Molecular Identification of Organic Compounds in the
615 Atmosphere: State of the Art and Challenges, *Chemical Reviews*, 115, 3919-3983,
616 10.1021/cr5003485, 2015.
- 617 Otkjær, R. V., Jakobsen, H. H., Tram, C. M., and Kjaergaard, H. G.: Calculated Hydrogen Shift Rate
618 Constants in Substituted Alkyl Peroxy Radicals, *The Journal of Physical Chemistry A*, 122, 8665-
619 8673, 10.1021/acs.jpca.8b06223, 2018.
- 620 Quéléver, L. L. J., Kristensen, K., Normann Jensen, L., Rosati, B., Teiwes, R., Daellenbach, K. R.,
621 Peräkylä, O., Roldin, P., Bossi, R., Pedersen, H. B., Glasius, M., Bilde, M., and Ehn, M.: Effect of
622 temperature on the formation of highly oxygenated organic molecules (HOMs) from alpha-
623 pinene ozonolysis, *Atmos. Chem. Phys.*, 19, 7609-7625, 10.5194/acp-19-7609-2019, 2019.
- 624 Savee, J. D., Papajak, E., Rotavera, B., Huang, H., Eskola, A. J., Welz, O., Sheps, L., Taatjes, C. A., Zádor,
625 J., and Osborn, D. L.: Carbon radicals. Direct observation and kinetics of a hydroperoxyalkyl
626 radical (QOOH), *Science*, 347, 643-646, 10.1126/science.aaa1495, 2015.
- 627 Seinfeld, J. H., and Pandis, S. N.: *Atmospheric Chemistry and Physics: From Air Pollution to Climate*
628 *Change*, 2nd ed., Wiley-Interscience, Hoboken, NJ, 1232 pp., 2006.
- 629 Smith, J. S., Laskin, A., and Laskin, J.: Molecular Characterization of Biomass Burning Aerosols Using
630 High-Resolution Mass Spectrometry, *Analytical Chemistry*, 81, 1512-1521, 10.1021/ac8020664,
631 2009.
- 632 Tomaz, S., Wang, D., Zabalegui, N., Li, D., Lamkaddam, H., Bachmeier, F., Vogel, A., Monge, M. E.,
633 Perrier, S., Baltensperger, U., George, C., Rissanen, M., Ehn, M., El Haddad, I., and Riva, M.:
634 Structures and reactivity of peroxy radicals and dimeric products revealed by online tandem
635 mass spectrometry, *Nature Communications*, 12, 300, 10.1038/s41467-020-20532-2, 2021.
- 636 Tröstl, J., Chuang, W. K., Gordon, H., Heinritzi, M., Yan, C., Molteni, U., Ahlm, L., Frege, C., Bianchi, F.,
637 Wagner, R., Simon, M., Lehtipalo, K., Williamson, C., Craven, J. S., Duplissy, J., Adamov, A.,
638 Almeida, J., Bernhammer, A.-K., Breitenlechner, M., Brilke, S., Dias, A., Ehrhart, S., Flagan, R. C.,
639 Franchin, A., Fuchs, C., Guida, R., Gysel, M., Hansel, A., Hoyle, C. R., Jokinen, T., Junninen, H.,
640 Kangasluoma, J., Keskinen, H., Kim, J., Krapf, M., Kürten, A., Laaksonen, A., Lawler, M.,
641 Leiminger, M., Mathot, S., Möhler, O., Nieminen, T., Onnela, A., Petäjä, T., Piel, F. M.,
642 Miettinen, P., Rissanen, M. P., Rondo, L., Sarnela, N., Schobesberger, S., Sengupta, K., Sipilä, M.,
643 Smith, J. N., Steiner, G., Tomè, A., Virtanen, A., Wagner, A. C., Weingartner, E., Wimmer, D.,
644 Winkler, P. M., Ye, P., Carslaw, K. S., Curtius, J., Dommen, J., Kirkby, J., Kulmala, M., Riipinen, I.,
645 Worsnop, D. R., Donahue, N. M., and Baltensperger, U.: The role of low-volatility organic
646 compounds in initial particle growth in the atmosphere, *Nature*, 533, 527-531,
647 10.1038/nature18271, 2016.
- 648 Van Krevelen, D. W.: Graphical-statistical method for the study of structure and reaction processes of
649 coal, *Fuel*, 29, 269-284, 1950.
- 650 Vereecken, L., Müller, J. F., and Peeters, J.: Low-volatility poly-oxygenates in the OH-initiated
651 atmospheric oxidation of α -pinene: impact of non-traditional peroxy radical chemistry,
652 *Physical Chemistry Chemical Physics*, 9, 5241-5248, 10.1039/B708023A, 2007.
- 653 Walser, M. L., Desyaterik, Y., Laskin, J., Laskin, A., and Nizkorodov, S. A.: High-resolution mass
654 spectrometric analysis of secondary organic aerosol produced by ozonation of limonene,
655 *Physical Chemistry Chemical Physics*, 10, 1009-1022, 10.1039/B712620D, 2008.
- 656 Wang, Z., Popolan-Vaida, D. M., Chen, B., Moshhammer, K., Mohamed, S. Y., Wang, H., Sioud, S., Raji,
657 M. A., Kohse-Höinghaus, K., Hansen, N., Dagaut, P., Leone, S. R., and Sarathy, S. M.: Unraveling
658 the structure and chemical mechanisms of highly oxygenated intermediates in oxidation of
659 organic compounds, *Proceedings of the National Academy of Sciences*, 114, 13102-13107,
660 10.1073/pnas.1707564114, 2017.
- 661 Wang, Z., Chen, B., Moshhammer, K., Popolan-Vaida, D. M., Sioud, S., Shankar, V. S. B., Vuilleumier, D.,
662 Tao, T., Ruwe, L., Bräuer, E., Hansen, N., Dagaut, P., Kohse-Höinghaus, K., Raji, M. A., and



22

- 663 Sarathy, S. M.: n-Heptane cool flame chemistry: Unraveling intermediate species measured in a
664 stirred reactor and motored engine, *Combustion and Flame*, 187, 199-216,
665 10.1016/j.combustflame.2017.09.003, 2018.
- 666 Wang, Z., Ehn, M., Rissanen, M. P., Garmash, O., Quéléver, L., Xing, L., Monge Palacios, M., Rantala,
667 P., Donahue, N. M., Berndt, T., and Sarathy, M.: - Efficient alkane oxidation under combustion
668 engine and atmospheric conditions, *Communications Chemistry*, 4, 10.1038/s42004-020-
669 00445-3, 2021.
- 670 Warscheid, B., and Hoffmann, T.: Structural elucidation of monoterpene oxidation products by ion
671 trap fragmentation using on-line atmospheric pressure chemical ionisation mass spectrometry
672 in the negative ion mode, *Rapid Communications in Mass Spectrometry*, 15, 2259-2272,
673 10.1002/rcm.504, 2001.
- 674 Witkowski, B., and Gierczak, T.: Characterization of the limonene oxidation products with liquid
675 chromatography coupled to the tandem mass spectrometry, *Atmospheric Environment*, 154,
676 297-307, /10.1016/j.atmosenv.2017.02.005, 2017.
- 677 Wotton, B. M., Gould, J. S., McCaw, W. L., Cheney, N. P., and Taylor, S. W.: Flame temperature and
678 residence time of fires in dry eucalypt forest, *International Journal of Wildland Fire*, 21, 270-
679 281, /10.1071/WF10127, 2012.
- 680 Xie, Q., Su, S., Chen, S., Xu, Y., Cao, D., Chen, J., Ren, L., Yue, S., Zhao, W., Sun, Y., Wang, Z., Tong, H.,
681 Su, H., Cheng, Y., Kawamura, K., Jiang, G., Liu, C. Q., and Fu, P.: Molecular characterization of
682 firework-related urban aerosols using Fourier transform ion cyclotron resonance mass
683 spectrometry, *Atmos. Chem. Phys.*, 20, 6803-6820, 10.5194/acp-20-6803-2020, 2020.
- 684 Zhang, H., Yee, L. D., Lee, B. H., Curtis, M. P., Worton, D. R., Isaacman-VanWertz, G., Offenber, J. H.,
685 Lewandowski, M., Kleindienst, T. E., Beaver, M. R., Holder, A. L., Lonneman, W. A., Docherty, K.
686 S., Jaoui, M., Pye, H. O. T., Hu, W., Day, D. A., Campuzano-Jost, P., Jimenez, J. L., Guo, H.,
687 Weber, R. J., de Gouw, J., Koss, A. R., Edgerton, E. S., Brune, W., Mohr, C., Lopez-Hilfiker, F. D.,
688 Lutz, A., Kreisberg, N. M., Spielman, S. R., Hering, S. V., Wilson, K. R., Thornton, J. A., and
689 Goldstein, A. H.: Monoterpenes are the largest source of summertime organic aerosol in the
690 southeastern United States, *Proceedings of the National Academy of Sciences*, 115, 2038-2043,
691 10.1073/pnas.1717513115, 2018.
- 692 Zhao, Y., Thornton, J. A., and Pye, H. O. T.: Quantitative constraints on autoxidation and dimer
693 formation from direct probing of monoterpene-derived peroxy radical chemistry, *Proc Natl
694 Acad Sci U S A*, 115, 12142-12147, 10.1073/pnas.1812147115, 2018.